22 August 1980, Volume 209, Number 4459 SCIENCE

The Einstein Observatory: New Perspectives in Astronomy

Riccardo Giacconi and Harvey Tananbaum

Summary. High-sensitivity x-ray measurements with the recently launched Einstein Observatory are having a major impact on wide areas of astronomical research. The x-ray luminosity of young O, B, and A stars and late K and M stars is found to be several orders of magnitude greater than predicted by current theories of coronal heating. Detailed x-ray images and spectra of supernova remnants are providing new information on the temperature, composition, and distribution of material ejected in supernova explosions as well as of the material comprising the interstellar medium. Observations of galaxies are yielding insights on the formation and evolution of stellar systems and galaxies over a wide range of variables. X-ray time variations are being used to probe the underlying energy source in quasars and active galactic nuclei. The distribution of mass in clusters of galaxies is being traced through detailed x-ray images, and the data are being used to classify clusters and trace their formation and evolution. Substantial progress is being made in several areas of cosmological research, particularly in the study of the diffuse x-ray background.

X-ray astronomy has become a major branch of observational astronomy since its beginning less than 20 years ago. The pace of discovery in this field can be compared to the great surge in radio astronomy over the past quarter-century.

The first exploratory phase occurred with rocket flights in the period 1962 to 1970 and with crude satellite instruments for exploratory surveys in the period 1970 to 1978. The astonishingly rich returns from even these relatively insensitive instruments were due in large part to the discovery of extremely luminous galactic and extragalactic x-ray sources whose existence was previously unsuspected. Perhaps most important among these results were the discovery of x-ray emission from mass-exchange binary systems containing a collapsed star (white dwarfs, neutron stars, and possibly black holes), which has provided us with a unique laboratory for the study of relativistic astrophysics, and the discovery of the intergalactic high-temperature gas associated with clusters of galaxies, a previously unobserved component of the universe containing as much luminous mass as all other known objects. The rich phenomenology of the high-energy sky revealed by these early missions had only little overlap with the interests of the mainstream of traditional astronomy, since only exceptionally luminous galactic sources and only the nearest and most powerful extragalactic sources could be observed.

The situation changed radically with the launch on 13 November 1978 of the Einstein (HEAO-2) Observatory, which introduced the use of focusing high-resolution optics to x-ray astronomy. The improvement in sensitivity and resolution brought about by this mission has resulted in a qualitative change in the scope of the discipline. At one stroke, x-ray observations have been extended to all known classes of stars in our galaxy and to the most distant discrete objects known in the universe. Although the analysis of the data is still in preliminary form, it is already clear that x-ray observations are again revealing new and unsuspected aspects of astronomical objects.

X-ray observations have emerged so rapidly as a powerful tool for astronomy because of the prevalence of high-energy phenomena in the universe and the important and at times determinant role that they play in its dynamics and evolution. This view of a universe in constant turmoil, created in an enormous initial explosion, with components being torn apart again and again by impulsive events, is one that has developed over the last few decades through observations at all wavelengths from the microwave band to the gamma-ray region of the spectrum—the highest energy radiation accessible for study. Modern astronomy has adopted an all-wavelength approach to the study of the heavens and to the extraction of crucial information about the processes that determine the evolution of stars and galaxies.

In particular, many of the violent processes of formation and collapse of stars and galaxies give rise to high-temperature gases or high-energy particles. When this occurs, copious x-ray fluxes are produced, either through thermal emission from gases with temperatures of millions of degrees or by interaction of the high-energy particles with electromagnetic fields or photons. The x-rays thus produced can readily traverse the vast interstellar and intergalactic distances separating us from their point of origin, although they cannot penetrate the earth's atmosphere. The development of space observatories has made it possible to use this rich new channel of information.

Riccardo Giacconi is a professor of astronomy at Harvard University and an associate director of the High Energy Astrophysics Division, Harvard/Smithsonian Center for Astrophysics, Cambridge, Massachusetts 02138. Harvey Tananbaum is a research scientist at the Harvard/Smithsonian Center for Astrophysics.

0036-8075/80/0822-0865$02.00/0

The Einstein Observatory

The first surveys and discoveries in x-ray astronomy were made primarily with mechanically collimated detectors. However, the sensitivity of these early observations fell short of that required to realize the full potential of x-ray astronomy for the study of low-luminosity objects in our galaxy, for the study of extragalactic objects, and for serious cosmological research. This limitation in sensitivity was essentially due to the background-limited nature of the instrumentation; sensitivity could increase only in proportion to the square root of the product of the detector area and the observing time. Further progress in the field required instruments built on entirely different principles.

At visible light and radio wavelengths, astronomers are well aware of the increase in sensitivity that results from the use of focusing optics. By concentrating the signal into a relatively small detector element, through focusing, the observer achieves a great reduction in background and increases the angular resolution as well. However, the application of this concept to x-ray astronomy is quite difficult, since under normal conditions lenses and mirrors tend to absorb rather than focus x-rays. It had been discovered in the 1930's that one could achieve high efficiency of reflection if x-rays were made to reflect from a surface at very small angles of incidence (grazing incidence). This effect is possible because the index of refraction of some materials is slightly smaller at x-ray wavelengths than the index in vacuum. Radiation incident at angles less than the critical angle (grazing angle) can therefore undergo total external reflection. By 1952 Wolter (*1*) had generated optical designs for an x-ray microscope based on this principle, but no practical implementation was possible because of the inability to polish the very small surfaces involved to the very high accuracies required. By 1960 Giacconi and Rossi (*2*) had recognized the great advantage that focusing optics could bring to x-ray astronomy, as well as the feasibility of constructing the required optical surfaces on the large physical scale appropriate for telescopes.

During the ensuing decade the required fabrication techniques and technology were developed and first applied to studies of the sun, culminating with the many thousands of highly resolved pictures of the solar corona which the astronauts brought back from Skylab (*3*). As a result of the developments in x-ray astronomy as a whole and in the use of focusing optics for solar studies, NASA accepted a 1970 proposal for an x-ray telescope mission to study extrasolar sources. This proposal was submitted by a consortium including Columbia University, Massachusetts Institute of Technology (MIT), Goddard Space Flight Center (GSFC), and our scientific group, then at American Science and Engineering and now at the Harvard-Smithsonian Center for Astrophysics (CFA). The mission was finally realized with the launch on 13 November 1978 of the Einstein Observatory.

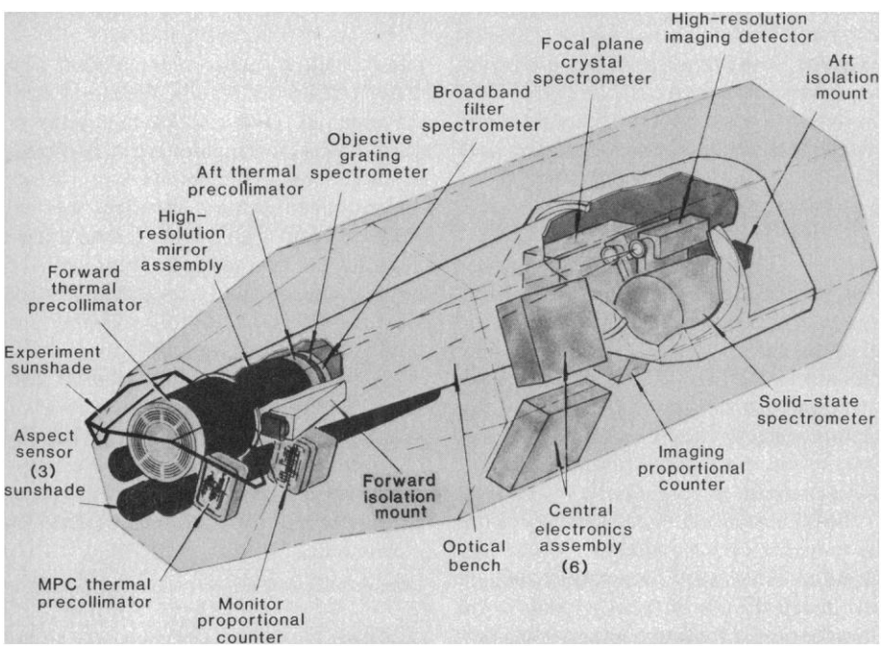

Fig. 1. Schematic diagram showing the major scientific elements comprising the Einstein Observatory. [This figure originally appeared in *Astrophysical Journal*]

The scientific portion of the satellite is diagrammed in Fig. 1, which shows the 0.6-meter-aperture x-ray telescope, the optical bench, and the focal plane transport assembly, a lazy-Susan arrangement that permits one of several imaging instruments or spectrometers to be brought to the focus (*4*). Three star sensors are flown for on-the-ground aspect determination and as part of the on-orbit attitude control system, which also utilizes gyroscopes, reaction wheels, and reaction control gas to unload momentum from the reaction wheels.

The grazing incidence telescope consists of four nested paraboloids of revolution followed by four nested hyperboloids. The nearly cylindrical surfaces are nested inside one another to increase the effective collecting area. The mirrors are made of fused quartz, which is figured and polished to very high precision. A very thin nickel coating provides the desired index of refraction for focusing the x-rays. Two reflections are required for each x-ray (one by a paraboloid and one by the following hyperboloid) to achieve a reasonable resolution over the 1° field of view of the telescope. At low energies (0.25 kiloelectron volts) the total effective area of the mirror is ~ 400 square centimeters, and this decreases to 30 square centimeters at the high-energy cutoff (4 kiloelectron volts). Since the grazing angles are $\lesssim 1°$, approximately 60×400 cm^2 of total surface area was actually figured and polished for the set of four paraboloids and four hyperboloids. The total area of each of these sets corresponds to slightly more than the area of the Hale Observatory–Mount Palomar 200-inch optical reflector.

Our group at CFA developed two types of complementary imaging detectors to employ at the focus of the telescope. A high-resolution imager (HRI) utilizes two multichannel plates operating in cascade to convert individual x-rays to an electron cloud, whose centroid is determined by using a crossed-grid charge detector and associated electronics. The position and time of each event (up to 100 per second) are inserted as digital data into the telemetry stream and can be combined with the aspect data on the ground to reconstruct the x-ray image of the sky. This detector has the highest spatial resolution available, 1 arc second, to be used in conjunction with the 3.5 arc second angular resolution (full width at half-maximum) of the telescope. It covers the central 25 arc minutes of the telescope field of view, has a detection quantum efficiency that varies from 30 to 6 percent over our energy band, and has no inherent spectral

resolution, although it can be used in conjunction with interchangeable broadband filters and transmission gratings that can be placed into the x-ray beam.

The second type of imaging detector is an imaging proportional counter (IPC), which has 1 arc minute spatial resolution, a 1° field of view to cover the full telescope aperture, a high-quantum efficiency, and moderate spectral resolution. Imaging is accomplished by use of two planes of cathode wires with an anode plane in between. An incident x-ray is converted to an electron, which creates an avalanche at the anode while still preserving spatial information. Induced signals are sensed on the cathodes and used to generate the position information.

The observatory also carries two sensitive spectrometers for use at the telescope focus. One is a cooled, solid-state silicon spectrometer developed by GSFC, which combines high efficiency with good resolution (~ 150 electron volts). The other is a curved crystal Bragg spectrometer developed by MIT, which features very high resolution (in some cases of order 1 eV) accompanied by relatively low efficiency.

Although Einstein was originally proposed and approved as a principal investigator experiment, we have long recognized the desirability of making its great capabilities available to all interested astronomers. Therefore, the observatory has been operated as a national facility since its launch, and more than 330 guest observers were approved during the first 1½ years. A series of guest and consortium observing targets, now numbering more than 7000, are entered and stored in our computer. Approximately ten different targets are selected each day so that more than 3000 have been observed in the first year. Commands are generated to configure and point the observatory for sequences approximately 12 hours long. Once per orbit the onboard tape recorder transmits ~ 100 minutes of data to a NASA ground station. These data are then relayed to GSFC and forwarded to the CFA. At the CFA a specialized data handling system is used to manipulate the data stream, determine the instantaneous pointing direction of the telescope as a function of time, and produce x-ray images of the sky. These images can then be searched for sources before further detailed scientific analyses are carried out. The data can also be displayed and manipulated on one of several television screens provided as part of the computer system.

The satellite has operated without serious problems since its launch and, as discussed below, has fulfilled our expectations with regard to increased sensitivity and angular resolution. The only serious limitation of the observatory is its finite lifetime. At the time of launch, the nominal lifetime was 1 year. Through judicious target scheduling designed to minimize net perturbing torques, we have been able to extend the life expectancy of the finite amount of gas available to remove momentum from the reaction wheels. At present we expect the gas to last through 1981—2 years beyond the nominal 1 year. It is also probable that the continued high level of solar activity will cause the satellite orbit to decay by 1982, leaving us without an ongoing high-sensitivity x-ray astronomy facility possibly until the launch of the Advanced X-ray Astrophysics Facility (AXAF) around 1987 or 1988.

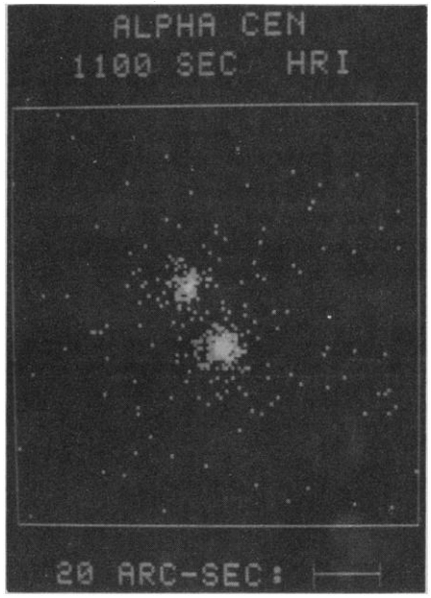

Fig. 2. High-resolution x-ray photograph of nearby binary star system, Alpha Centauri. The brighter x-ray source corresponds to the K star and the other x-ray source to the G star, contrary to theoretical expectations for the relative x-ray emission from these two different classes of stars.

X-rays from Stellar Systems

Considerable progress has been made in the last 50 years in understanding the formation and evolution of stars, particularly during the long period of time they spend in the quiet burning of their nuclear fuels after they reach the main sequence. However, the answers to many important problems remain incomplete. These include the details of the stellar formation process, of the energy transport processes in main sequence stars, of the collapse of massive stars, and of the behavior of matter in superdense collapsed stars.

The full range of these problems is being attacked by astronomers, using all the observational tools at their disposal. For example, infrared observations have given us the opportunity to study many aspects of the early phases of stellar evolution (*5*). Spectroscopic studies in the visible range of wavelengths and more recently in the ultraviolet from the Copernicus satellite have provided fundamental clues to the behavior of stars throughout their evolutionary track (*6*).

In its first decade, x-ray astronomy appeared to be mainly capable of giving information about the later stages of stellar evolution. The discovery by UHURU of binary x-ray sources (*7*), which contain a collapsed star accreting matter from its normal companion, provided startling new information regarding the endpoints of stellar evolution. It first demonstrated that the formation of a neutron star (presumably through a supernova explosion) need not disrupt the binary system in which the star is contained. It provided an astrophysical laboratory in which the properties of the collapsed object itself could be studied as they manifested themselves in response to varying torques and forces due to changes in the accretion flow. The internal structure of neutron stars could be studied and their angular momentum, crust-to-core coupling, and other characteristics measured.

The binary x-ray systems provided the first independent measurements of neutron star masses. For one system, Cygnus X-1, combined x-ray and optical observations revealed the existence of a compact object less than 10 kilometers in radius with a mass of more than 6 solar masses and incompatible with any equilibrium solution predicted by general relativity except for a black hole. Cygnus X-1 still furnishes the most promising and convincing evidence we have for the existence of black holes of stellar mass (*8*).

The discovery of x-ray bursts (*9*) with the ANS satellite led to an intensive study of these objects by SAS-3, HEAO-1, and most recently Hakucho, the Japanese x-ray satellite. In these systems the general characteristics of the luminous x-ray sources described above, namely their very high absolute luminosity (~ 10^{37} to 10^{38} ergs per second) and very rapid time variability, appear to be carried to an extreme. Extremely luminous (10^{38} to 10^{40} erg/sec) flashes of radiation appear to originate from otherwise inconspicuous objects located sometimes in the center of globular clus-

ters but often outside as well. Although we still cannot fully decide between models involving massive accreting black holes and binary systems containing a neutron star, the present consensus seems to prefer the latter interpretation; in that case these objects would be of the same general class as the binaries previously described. With the HEAO-1 spacecraft other types of lower luminosity binaries, such as RS CVn systems containing a K star and a G star, were discovered to be x-ray emitters. A few lower luminosity binaries containing white dwarf secondaries had also been detected as x-ray sources by rocket and satellite experiments, as had a few isolated stars (*10*).

With its qualitative improvement in sensitivity, the Einstein Observatory has brought about a revolutionary change in the prospects for stellar studies through x-ray observations. All classes of known stars have now been detected in their x-ray light (*11*), with x-ray luminosities ranging from 10^{26} to 10^{34} erg/sec. The predictions for main sequence stars based on coronal heating mechanisms through the acoustic noise of convective motions have been found to be widely at odds with observations. From young stars of the O, B, and A spectral types, as well as from the late K and M stars, the observed x-ray fluxes are 1000 to 1 million times greater than expected. Figure 2 shows, for example, an IPC image of Alpha Centauri. The x-ray emission from the K star is found to be more intense than that from the G star, contrary to theoretical expectation. In Fig. 3 the observed ratio of the x-ray to visible light flux is shown as a function of spectral type (as well as blue color excess in the visible) for main sequence stars. Previous theoretical calculations based primarily on our knowledge of one star, the sun, predicted substantial x-ray fluxes only for late A, F, and G stars, whereas the observations show substantial x-ray emission for all spectral types. These findings will form the foundation for new theoretical modeling of the energy transport mechanisms from the core and heating of the outer atmosphere of stars. We suspect that any new model will have to take fully into account the roles of the magnetic field and of stellar rotation.

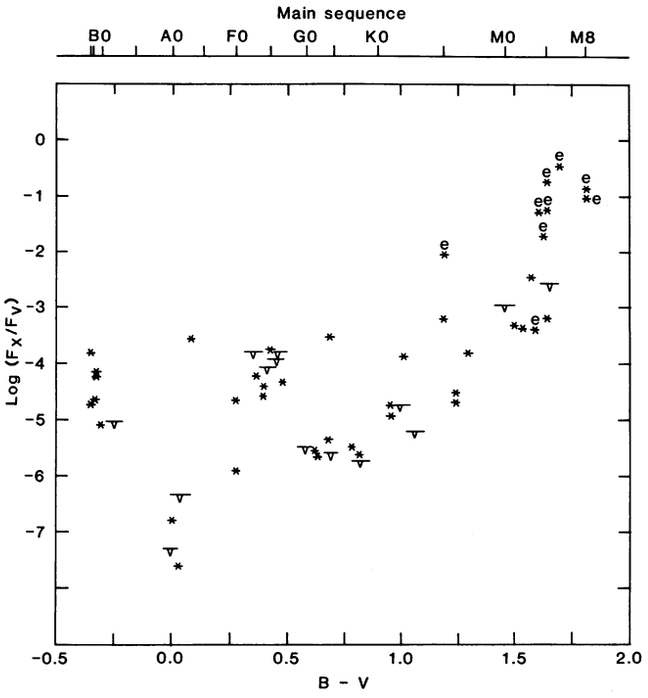

Fig. 3. Ratio of x-ray to visible light flux plotted logarithmically against (visible light) spectral type to summarize the Einstein x-ray observations for various main sequence stars. Spectral type ranges from O and B stars, which are the hottest, bluest, and youngest, to M stars, which are the coolest, reddest, and oldest. The $B-V$ scale is a visible light color difference index. For several stars not detected in the x-ray observations, upper limits are indicated.

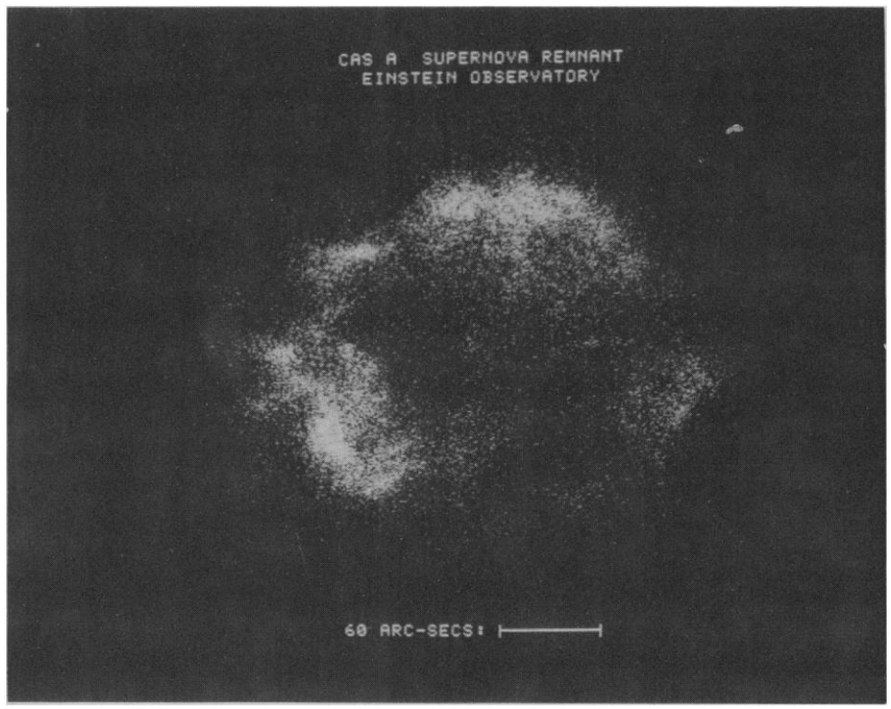

Fig. 4. High-resolution x-ray image of the shell-like supernova remnant Cas A. Various features seen in this image are discussed in the text. The data are digitized into 2 arc second by 2 arc second pixels (picture elements), and the overall exposure time is ~ 30,000 seconds.

For early stars and stars possibly still embedded in their parent nebulas the Einstein observations also seem to open a new avenue of study. The discovery of x-ray emission from young O and B stars in associations (*12*), from the Orion variables and the stars in the Orion Trapezium (*13*), from the Eta Carinae nebula (*14*), and other peculiar objects show that high-energy photons are produced at the seat of stellar formation and can reach us through the gaseous envelope that prevents us from seeing the objects in visible light. If stellar winds furnish the means of shedding excess material and if bubbling up and annihilation of magnetic fields furnish the means of removing magnetic energy and possibly angular momentum, we can expect x-ray observations to provide crucial clues to the formation process of stars in the pre-main sequence period.

Important new information has also been provided by the Einstein Observatory on the remnants of supernova explosions. In some of them the burnt cinder of the explosion, a pulsar, can easily be detected. The cover, for example, shows an x-ray picture of the Crab Nebula pulsar and the surrounding nebulosity. The entire x-ray emission in this case

appears to be powered by high-energy electrons accelerated in the high magnetic field of the spinning neutron star. As the electrons interact with the surrounding magnetic field, they produce the observed x-rays by synchrotron emission. No trace is seen of the external layers of the star presumably blown off in the explosion that created the pulsar. The two parts of the cover picture are time-phased x-ray photographs comprised of data folded with the 33-millisecond period of the Crab pulsar. Each photograph represents 10 percent of the period summed over many cycles. For the data centered on the main pulse (phase 0.0) the pulsar is very bright (overexposed) and dominates the picture, while for the data centered off the pulse (phase 0.6) only a very weak point component is found at the pulsar location (*15*). By using the data away from the main and secondary pulses, we can search for steady, blackbody emission from the surface of the rotating neutron star. Our preliminary analysis indicates that the weak point emission during the off phase corresponds to 1.4×10^{34} erg/sec in the energy range 0.1 to 4 keV, which corresponds to a temperature of about 2.5 million kelvins if we assume blackbody emission from a neutron star with radius 10 km. Even if the off-state emission is not from the neutron star surface, these data set an upper limit for blackbody emission and require rapid cooling for the Crab neutron star.

It is also quite interesting that no evidence has yet been found for pulsed or unpulsed emission from a neutron star at the center of any of the historic supernovas except for Crab and Vela. We are left wondering whether a supernova explosion must always result in the production of a pulsar or, if this is the case, whether more efficient cooling mechanisms than neutrino cooling may make the pulsar undetectable (*16*). Pion cooling has been suggested, for example, to explain the possibility that the neutron star may be so cold as to no longer be detectable at x-ray wavelengths.

Some of the historical supernova remnants, such as SN 1006, Tycho, and Cassiopeia A, have an appearance very different from the Crab, with the x-ray emission showing a well-developed shell structure. The HRI image of Cas A is shown in Fig. 4. We are able to recognize several regions of x-ray emission: (i) an emission shell lying outside the region of the optical filaments, due presumably to the interaction of the shock front with the interstellar material; (ii) a region associated with fast-moving knots from which material may be either evaporated due to heating by the shock or ablated due to the passage of these knots in the interstellar medium (the material of the knots was presumably ejected during the supernova explosion itself); (iii) a region of x-ray emission associated with stationary flocculi, possibly the remains of material ejected from a star prior to the explosion and heated to x-ray temperatures by the shock; and (iv) a region connected with radio emission, presumably from high-energy electrons spiraling in the local magnetic field and producing x-rays by nonthermal processes. From a preliminary analysis the total amount of mass involved in the supernova can be estimated as 10 to 30 solar masses (*17*).

Spectroscopic observations by the GSFC group with the solid-state spectrometer on the Einstein Observatory provide detailed information on the elemental composition and temperature of the material blown off in the explosion (*18*). A spectrum of a large region in the Cas A supernova shell is shown in Fig. 5. The data show substantial line emission consistent with transitions of helium-like ions of silicon, sulfur, and argon with abundances ranging from 1.7 to 6.9 times the solar abundances. The helium-like nature of the transitions limits the temperature in the emitting region to less than 10×10^6 K. The absence of excess iron group material suggests that at the time of the explosion the stellar core had not yet advanced to the stage of substantial burning of silicon group material to form iron group material. The data also support models in which the iron group material formed in the supernova explosion is located close to the center and is ejected less forcefully than the silicon group material. As a result, the more slowly expanding iron group material is located to the inside of the silicon-rich shell we observe and has not yet been reheated to x-ray–emitting temperatures by the inward-moving reverse shock (*19*).

Even from the preliminary account of the supernova observations made possible by the imaging techniques and high sensitivity of Einstein, it is apparent that spectrally resolved x-ray images of such explosive events may give us a unique tool for studying pre- as well as post-supernova conditions. Far from being a bizarre and rare event, supernovas are the factory where the heavy elements are manufactured and dispersed into the interstellar medium. The transfer of the kinetic energy of the explosions determines the temperature of the interstellar medium. It is clear that the x-ray contribution to our understanding of these events will noticeably advance our knowledge of stellar evolutionary processes.

X-ray Emission from Galaxies

Over the past 50 years, visible light and radio observations have identified characteristic properties that have been used to classify galaxies and to investigate their formation and development. For example, "normal" galaxies have

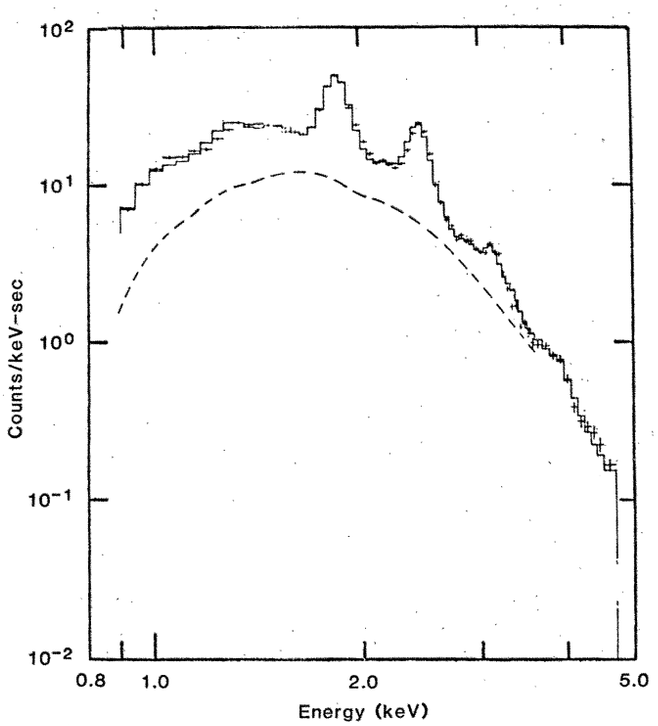

Fig. 5. Solid-state spectrometer observations of Cas A, showing the spectrum for the overall x-ray source in the energy band 0.9 to 4.5 keV. The lower dashed curve represents the continuum contribution from hydrogen, helium, carbon, nitrogen, oxygen, and neon components of the hot gas. The total emission (top curve) is comprised of this continuum plus line emission from magnesium, aluminum, silicon, sulfur, argon, calcium, and iron. The three largest peaks in the top curve are associated with silicon, sulfur, and argon. [Courtesy of S. S. Holt; this figure originally appeared in *Astrophysical Journal*]

been described as elliptical, spiral, or irregular with several subclasses on the basis of their optical morphology. The presence of a very bright nucleus in a faint galaxy has been a primary signature for a Seyfert galaxy. Spectroscopic observations of broad hydrogen lines and broad forbidden lines (widths $\gtrsim$ 1000 km/sec) have been used to characterize a subset of Seyfert galaxies as type 2, while Seyferts with hydrogen line widths of order 10,000 km/sec have been called type 1 (*20*). Similar spectra with very broad emission lines characterize the quasars (quasi-stellar objects, or QSO's), although surrounding faint nebulosities have, in general, not yet been detected for these objects, perhaps because they are considerably more distant than most Seyfert galaxies. Another class of galaxies recently identified and thought to be related to quasars are the BL Lacertae objects. BL Lacs are characterized by weak or absent emission lines, rapid optical variability, strong and variable optical polarization, and radio emission. Among the other categories of galaxies that have been established are those characterized by narrow emission lines, radio galaxies, and N-type galaxies.

This great variety of characteristics raises many questions about the formation and evolution of galaxies and about the relationships between different morphological types. When did galaxies first form? How do the gas content, stellar content, and morphological classification evolve as a function of time for different types of normal galaxies? Are type 1 Seyfert galaxies and normal galaxies remnants of quasars that were more luminous at an earlier time? In addition to these types of questions, a very basic unknown is the nature of the central energy source that powers the nuclei of normal and active galaxies, including quasars.

While still in a relatively early stage of development, our studies of the x-ray-emitting properties of galaxies can now be directed toward these questions. As described earlier, the x-ray emission from our own galaxy is comprised of several elements including mass-exchange binary systems, supernova remnants, and normal stars, as well as an overall diffuse component arising from hot interstellar gas. Our observations of nearby normal galaxies provide information on these same phenomena, but with the additional feature of having all of the sources for a given galaxy at essentially the same, known distance.

Thus the Einstein observations of 13 supernova remnants in the Large Magellanic Cloud (at a distance of 55,000 parsecs, or 180,000 light-years) have permitted our colleagues at Columbia University (*21*) to determine the x-ray luminosities and in several cases the remnant temperature and x-ray shell size. These observations have been combined with radio and optical data, and the Sedov solution for a symmetrical blast wave propagating into the interstellar medium has been used to solve for the age of the remnants, the initial energies in the supernova explosions, and the ambient densities of the interstellar medium. The Columbia group finds that the ages range from 1,000 to 20,000 years; the initial energies range from 0.8×10^{50} to 3.4×10^{50} ergs, similar to energies derived for supernovas in our galaxy; and the interstellar medium densities range from 5×10^{-2} to 10 cm^{-3}. They find that the densities are highly correlated with observed remnant diameters; this correlation is not consistent with a simple blast wave propagating into a homogeneous medium. A lower density interstellar medium studded with higher density clouds might fit the observed correlation between density and diameter in a reasonable manner.

Another example of a normal galaxy is provided by our twin, M31 or Andromeda. At a distance of ~ 700,000 parsecs (~ 2 million light-years), M31 occupies a region of about 2° on the sky, and several x-ray observations have to be combined in a mosaic to obtain an overall picture of the galaxy. At least 80 individual x-ray sources have been resolved in the combined HRI-IPC Einstein data (*22*), whereas previous observations were able to detect as a very faint source only the integrated emission from M31 as a whole. The individual sources observed by Einstein have luminosities of at least 9×10^{36} erg/sec and are probably mass-exchange binaries in most instances, although at least one supernova remnant has been identified. Individual normal stars would be too faint for us to detect, and the data have not been analyzed for extended interstellar emission. Many of the luminous x-ray sources are associated with the spiral arm structure of M31. Spiral arms are regions containing much gas and dust and are bright because many young, massive stars are being formed. Such conditions are conducive to the formation of massive binaries that eventually evolve into mass-exchange binary x-ray sources.

In the HRI image of the central region of M31 shown in Fig. 6, the outermost sources are probably associated with gas, dust, and spiral arm features. However, the 20 or so sources located within a central radius of 2 arc minutes may

Fig. 6. High-resolution imager exposure to the center of M31. North is to the top, east to the left. The many individual x-ray sources are apparent. On the basis of the observed x-ray luminosities, we believe that most of these sources are mass-exchange binary systems containing a collapsed star accreting gas from its companion.

well be a separate "inner bulge" population. These sources, as well as nine or ten probably associated with globular cluster systems in M31, may represent a different class of sources possibly connected with older, low-mass binary systems formed by a capture process. The average luminosity of the inner bulge sources in M31 is 4.5×10^{37} erg/sec, approximately twice the average luminosity of the spiral arm sources. More important, this inner bulge region, with a 400-parsec radius, contains about 1.5 percent of the mass of M31 and is responsible for ~ 33 percent of the 0.5- to 4.5-keV x-ray emission. It is also very much smaller than the inner bulge region of x-ray sources in our own galaxy. This concentration of x-ray–emitting systems in the center of M31 and the large x-ray output from a relatively small fraction of the galaxy's mass indicate that further x-ray studies of M31 and other nearby normal galaxies can teach us much more about the stellar evolutionary processes at work in different galaxies.

In addition to using observations of luminous binaries to study normal galaxies, we can apply observations of normal stars to study the stellar content of galaxies. For example, some models for elliptical galaxies invoke a population of M stars of low mass and low optical luminosity to account for a substantial fraction of the overall mass of the galaxy. For a galaxy containing 10^{11} to 10^{12} M stars we would expect an x-ray emission of 10^{38} to 10^{40} erg/sec from these stars alone. Einstein observations can detect such galaxies at least out to the Virgo cluster of galaxies (a distance of 20 million parsecs) and may provide the means of detecting the optically dark halos theorized to surround galaxies and comprise much of their mass.

The Einstein x-ray observations of the radio galaxy Centaurus A, located at a distance of 5 million parsecs, illustrate several different phenomena (*23*). A point x-ray source is associated with the nucleus of the galaxy. Extended x-ray emission has also been detected from a region 2 arc minutes in radius around the nucleus. This emission may be due to the superposition of presently unresolved luminous binaries or to a cloud of hot gas in the interior of the galaxy. Still farther away from the nucleus, x-ray emission is detected from the radio-emitting regions known as the inner lobes. Centaurus A shows two pairs of radio lobes aligned on opposite sides of the nucleus and thought to have been ejected in two separate explosive events. The data suggest that the x-ray emission from the inner lobes is produced by inverse Compton scattering of the radio-producing electrons off the photons responsible for the 3 K blackbody background. This then permits a first determination of the magnetic field for this region, which we calculate as 4×10^{-6} gauss.

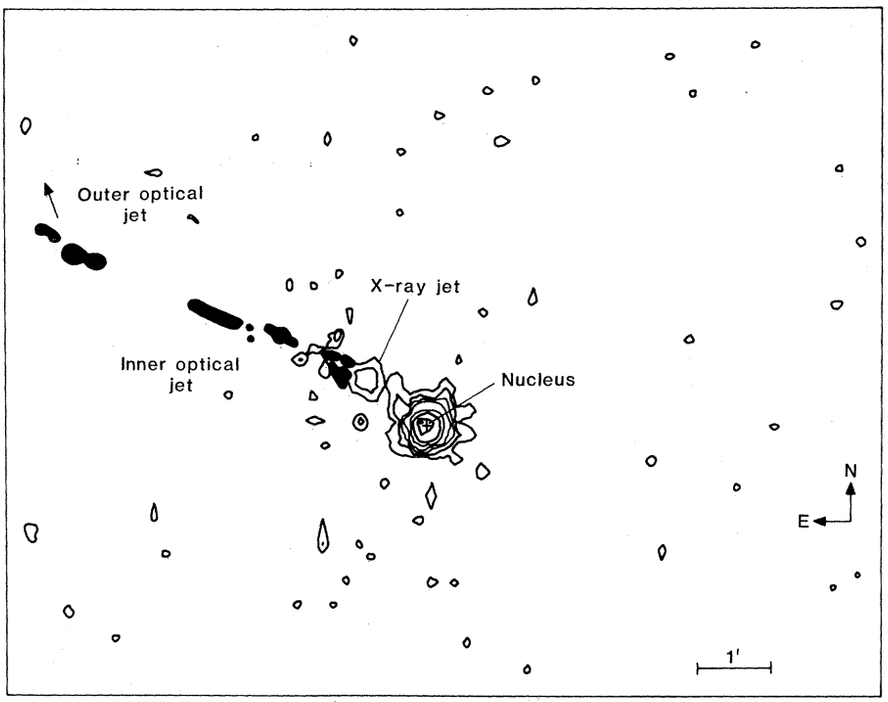

Fig. 7. Isointensity contour map of the HRI x-ray image obtained around the nucleus of the radio galaxy Centaurus A. The nucleus and x-ray jet toward the northeast are indicated, as is the optical jet. [This figure originally appeared in *Astrophysical Journal*]

Figure 7 is an isointensity contour plot of the HRI observations of Centaurus A, showing the pointlike source associated with the nucleus and an additional jetlike x-ray feature to the northeast of the nucleus. This x-ray jet is aligned with, but just within, a previously reported optical jet (*24*), and both are aligned in the direction of one of the inner radio lobes. Our calculations indicate that the x-ray emission in the jet can arise from thermal bremsstrahlung radiation, produced by the Coulomb acceleration of the hot electrons in the plasma. At the same time, the kinetic energy carried by the dense subrelativistic plasma comprising the jet is sufficient to power the inner radio lobe, which may resolve the question of the energy supply required by such long-lived radio-emitting regions.

In our description of x-ray emission from normal galaxies, we separate the galactic nucleus from the remainder of the galactic emission. It may well be that the emission from the nuclei of normal galaxies is closely related to the emission from the nuclei of active galaxies and quasars. Many astrophysicists believe that the nuclei of active galaxies are the sites of massive black holes and that the emission from these objects is powered by the gravitational energy released by infalling matter (*25*). One way of providing the infalling material is through tidal disruption of stars that wander too close to the black hole. Normal galactic nuclei might contain "dormant" or "fossil" black holes, which are quiet because of the temporary or permanent absence of infalling material. X-ray luminosities for galactic nuclei range from 10^{35} erg/sec for our galactic nucleus to 10^{38} erg/sec for M31, 10^{42} to 10^{45} erg/sec for type 1 Seyfert galaxies, and 10^{43} to 10^{47} erg/sec for quasars. Narrow-emission-line galaxies, type 2 Seyfert galaxies, radio galaxies, N-type galaxies, and BL Lacs also fit within this range. Thus the x-ray luminosities may be useful in establishing specific relationships among these various classes of active galactic nuclei. In the context of the massive black hole model, the observed luminosity can be used to estimate a minimum black hole mass through the Eddington limit, which establishes a maximum rate for the infalling gas due to the pressure created by the outward-moving radiation. For a 10^{47} erg/sec source, a minimum black hole mass of 10^9 solar masses is required.

Additional evidence that the activity in galactic nuclei occurs in very small regions was obtained by monitoring source intensities as a function of time. It now appears that our x-ray observations are capable of probing the innermost (or

smallest) regions of active galaxies and quasars. The data shown in Fig. 8 were obtained during a 2-day Einstein IPC observation of the Seyfert galaxy NGC 6814 (*26*). The data have been summed in 2000-second intervals and the count rate (in counts per 100 seconds) is plotted against time. Since the background count rate is monitored simultaneously elsewhere in the imaging detector (at less than 1 count per 100 seconds), we can be confident that the intensity variations seen in Fig. 8 are not due to background changes or instrumental effects. The error bars indicate the uncertainty in the count rate based on the actual number of counts. The mean for all of the data is shown by the dashed line. A chi-squared test indicates a negligible probability that the source intensity is constant. The data point at ~ 40 ksec is 5 standard deviations above the mean, indicating that significant changes occur in times no greater than 20,000 seconds. The average x-ray luminosity for this source is 4×10^{42} erg/sec and the observed variations indicate that a substantial fraction of this luminosity is produced in a region no more than 1/4 light-day in size. Similar variability has been observed in several type 1 Seyfert galaxies and quasars, although it has not been found in several others. Our findings of high luminosities and small x-ray-emitting regions, along with optical data showing high luminosities and rapid variability in some BL Lac objects and "violently variable" quasars, may be the most compelling evidence to date for the existence of massive black holes in active galactic nuclei.

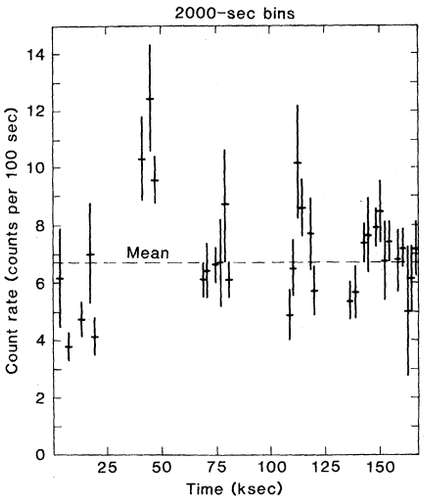

Fig. 8. X-ray intensity plotted in 2000-second intervals as a function of time for the type 1 Seyfert galaxy NGC 6814. The mean counting rate for the 2 days data is shown by the dashed line. Significant intensity variations are apparent in the data.

X-ray Emission from Clusters of Galaxies

As is well known, stars are not uniformly or randomly dispersed in space, but are aggregated along with gas and dust to form galaxies. In a somewhat similar fashion, galaxies are not uniformly distributed, but tend to occur in groups or clusters with tens to thousands of members in regions of space typically a few million light-years across. In addition to their component galaxies, clusters also contain substantial amounts of hot gas, as was first conclusively demonstrated by the UHURU observations of extended x-ray emission from clusters (*27*). The Einstein observations of clusters have been directed toward improving our understanding of how the cluster environment affects the evolution of individual galaxies and how the clusters as a whole form and evolve.

Our studies of the development of individual galaxies in a cluster environment are perhaps best illustrated by the x-ray results obtained for a portion of the Virgo cluster of galaxies, shown in Fig. 9 (*28*). Here we have plotted the isointensity x-ray contours superimposed on a visible light photograph (from the Kitt Peak 4-m telescope). The two brightest galaxies, the ellipticals M86 and M84, are both relatively bright x-ray sources. X-ray emission is also observed from the tidally disrupted galaxy NGC 4438 to the northeast and from the narrow-emission-line galaxy NGC 4388 to the southwest. Since M84 is a radio galaxy, we initially hypothesized that the x-ray emission might be related to activity in the galaxy nucleus. Subsequent observations with the Einstein HRI, utilizing the arc-second resolution capability, demonstrated that the x-ray emission from M84 is diffuse and not primarily associated with the nucleus of the galaxy. Our present understanding of the x-ray emission from M84 is probably best discussed in the context of the M86 data.

The contours in Fig. 9 for M86 show that the x-ray emission is extended over several arc minutes with an apparent asymmetry to the northeast. A preliminary spectral analysis of this extended emission indicates that it is produced by hot gas with a temperature of $\sim 10 \times 10^6$ K. From the observed x-ray luminosity of 2×10^{41} erg/sec and the temperature and size, we can compute the central particle density as $\sim 4 \times 10^{-3}$ cm^{-3}. This leads to a mass estimate of several billion solar masses for the x-ray-emitting gas. This gas is thought to be generated by mass lost from stars and heated by supernova explosions within the galaxy itself. If the overall mass of M86 is 10^{12} solar masses, then this hot x-ray-emitting gas cannot be completely bound gravitationally to the galaxy. Recent calculations (*29*) suggest that the gas may be confined by the external pressure generated by the hotter, lower density gas that has been observed through its x-ray emission to fill the Virgo cluster. The cooling time for this hot, low-density intracluster gas is greater than the age of the universe, which rules it out as the source of the x-ray emission from M86.

The confinement of the gas associated with M86 by the hotter, lower density cluster gas must compete with ram pressure forces trying to strip the gas from the galaxy as it moves through the cluster. Since M86 is probably in an eccentric orbit, it has spent much of its time moving at relatively low velocity far from the center of the Virgo cluster. Thus a stripping-free time of up to 5 billion years has been available to generate the gas that we are now observing. As M86 moves at higher velocity through the cluster core, most of this gas associated with the galaxy will be decelerated and stripped away by the ram pressure of the intracluster gas. On the other hand, M84 is a well-bound member of the Virgo cluster core, spending most of its time in the denser central region of the cluster. In this case the gas produced in the galaxy is continually stripped from all but the innermost regions, which explains the much smaller size observed in x-rays for M84.

It is interesting to note that the intracluster gas exerts two opposing effects on the gas produced in these elliptical galaxies. On the one hand, the tenuous external medium provided by the cluster gas may be sufficient to confine the gas and prevent its being lost from the galaxy. On the other hand, when the galaxy moves through a sufficiently dense part of the intracluster gas at sufficiently high velocity, the gas will be stripped from the galaxy. It is likely that this gas stripped from the galaxies is subsequently heated to become part of the hot intracluster gas, which is further discussed below. By comparison, we expect that gas generated in isolated elliptical galaxies will be lost from these galaxies through a galactic wind in the absence of the confining pressure of the intracluster medium unless very massive dark halos are present to gravitationally bind the gas. As mentioned above, x-ray observations have the potential for detecting low-mass M stars, which may comprise such massive halos, as well as the hot gas that would be bound.

This capability for detecting hot gas makes x-ray observations a most sensitive probe of the intracluster medium and thereby of the gravitational potential of the cluster as a whole. Various scenarios have been developed to describe the formation and evolution of clusters of galaxies, and we can use our x-ray data to evaluate these different formulations. An example of a cluster believed to be in an early phase of its development is shown in Fig. 10 (*30*). This is the cluster Abell 1367 at a distance of about 120 million parsecs. The x-ray emission is several times 10^{43} erg/sec and the isointensity contours shown in Fig. 10 demonstrate the broad, highly clumped nature of the emission. The x-ray picture is superimposed on an optical photograph and some of the x-ray peaks are associated with bright galaxies in the cluster, much as was the case for the Virgo cluster galaxies. In both of these examples we believe that the x-ray emission is dominated by gas that originates in the individual galaxies and is still at least partially bound to the galaxies. The gravitational potential of these individual galaxies is apparently more important for containment than the gravitational potential of the entire cluster. The galaxies move about the cluster with relatively low velocities and the gas temperature is also relatively low—about 15×10^6 K for Abell 1367. In some instances Fig. 10 shows x-ray enhancements or clumps of hot gas where no bright optical galaxy is present. We are scheduling higher resolution x-ray observations for this cluster to pursue the possibility that the x-ray enhancements are indicators of optically dark, previously undetected mass concentrations.

As the cluster continues to evolve, gas generated in the galaxies will be stripped by processes such as we discussed above for M86. This may affect the distribution of morphological types of galaxies in the clusters, with fewer gas-rich spiral galaxies in more highly evolved clusters. With the passage of time the gas and galaxies will interact with each other and a smooth, centralized distribution will develop following the cluster gravitational potential. Figure 11 shows the x-ray isointensity contours superimposed on an optical photograph of the cluster Abell 85, which we believe to be in this more highly evolved state. The data show a smooth, centrally peaked x-ray distribution, indicating that the gas distribution is, in fact, dominated by the overall cluster gravitational potential. The x-ray temperature for this cluster is at least 100×10^6 K, and the relative velocities of the galaxies are also expected to be high. The optical data also show a very bright central dominant (cD) galaxy at the cluster center. The formation of such a massive, bright galaxy may be enhanced by the high density of galaxies and/or gas in the cluster core, although not all highly evolved clusters contain such a cD galaxy. Further cluster evolution may lead to a smooth but somewhat relaxed or less concentrated distribution of gas and galaxies, which will also be reflected by the x-ray morphology. Examples of such clusters may be the Coma cluster, Abell 2319, and Abell 2256.

These models suggest a trend toward increasing cluster x-ray luminosity and temperature as a function of time, since the amount of gas available is increasing and the strength of the central gravitational potential is also increasing with time. In addition, gas that has been pro-

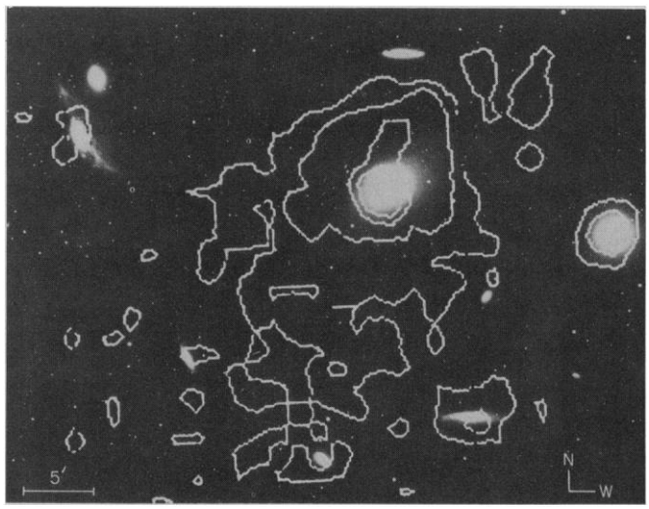

Fig. 9. Isointensity IPC x-ray data superimposed on a Kitt Peak 4-m visible light photograph of a portion of the Virgo cluster of galaxies. Extended x-ray emission associated with galaxy M86 is apparent, as are sources associated with galaxies M84, NGC 4438, and NGC 4388. [This figure originally appeared in *Astrophysical Journal*]

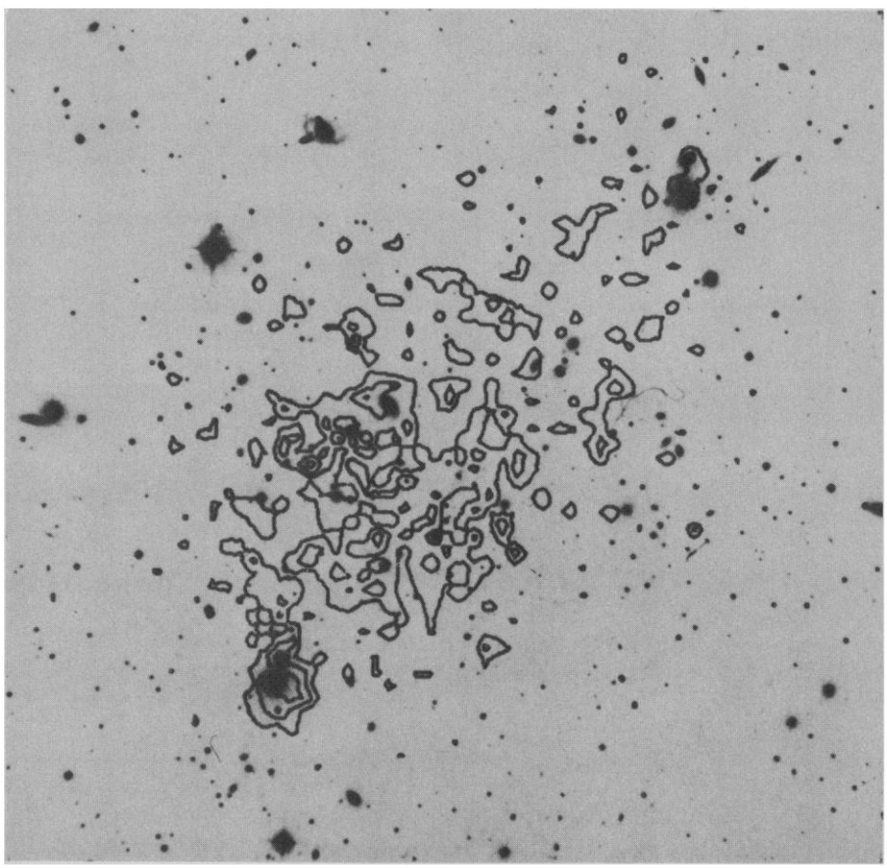

Fig. 10. Isointensity contour map of IPC x-ray data for cluster Abell 1367 superimposed on visible light photograph. Note the broad, highly clumped nature of the x-ray emission. [This figure originally appeared in *Astrophysical Journal*]

cessed through stars in galaxies and then released into the intracluster medium has been observed to be enriched in iron, with detectable iron emission lines in the x-ray spectra. This evolutionary picture can be tested in a statistical manner by observing the x-ray emission from a number of clusters at great distances (or large redshifts) and comparing it with data for relatively nearby clusters. On the average, clusters at large distances will appear earlier in their development than nearby clusters, since the radiation we observe now has taken millions or even billions of years to reach us. With Einstein we have initiated such an observing program. We have already detected some of the most distant known clusters out to a redshift (z) of 0.8, which corresponds to a distance of $\sim$ 5000 million parsecs (*31*). Although we have not yet obtained sufficient data to conclusively test the picture, the data obtained so far are consistent with this evolutionary scenario. More sensitive observations with an x-ray observatory following Einstein will be required to accurately map the cluster gas distribution in very distant clusters and to determine the iron content and spatial distribution in these clusters. It is also possible that this next-generation x-ray telescope will be capable of determining the largest redshift at which clusters exist and thereby establishing the age of the universe at which the clusters first formed.

Since the mass of the x-ray–emitting gas in the clusters is usually at least as large as the mass corresponding to the visible galaxies in the clusters, we can see the importance of using x-ray observations to trace the gas and determine its mass distribution and total mass. One of the more puzzling questions in astronomy involves the so-called missing mass in clusters. Observations of galactic velocities indicate that the mass required to keep the clusters bound exceeds the mass corresponding to visible galaxies by as much as a factor of 10. One possible explanation was that the missing mass was in the form of gas. While the x-ray observations confirm the presence of considerable amounts of gas, there is still not enough in the core of the cluster to hold the cluster together. Substantially more gas may exist outside the cluster core although the contribution of such gas to the binding of the cluster is still the subject of some controversy. Another possibility is that the missing mass may exist in dark, massive halos of individual galaxies, a possibility that we discussed earlier. In each of these cases the x-ray data will be required to provide critical detailed information on the distribution of matter within the clusters.

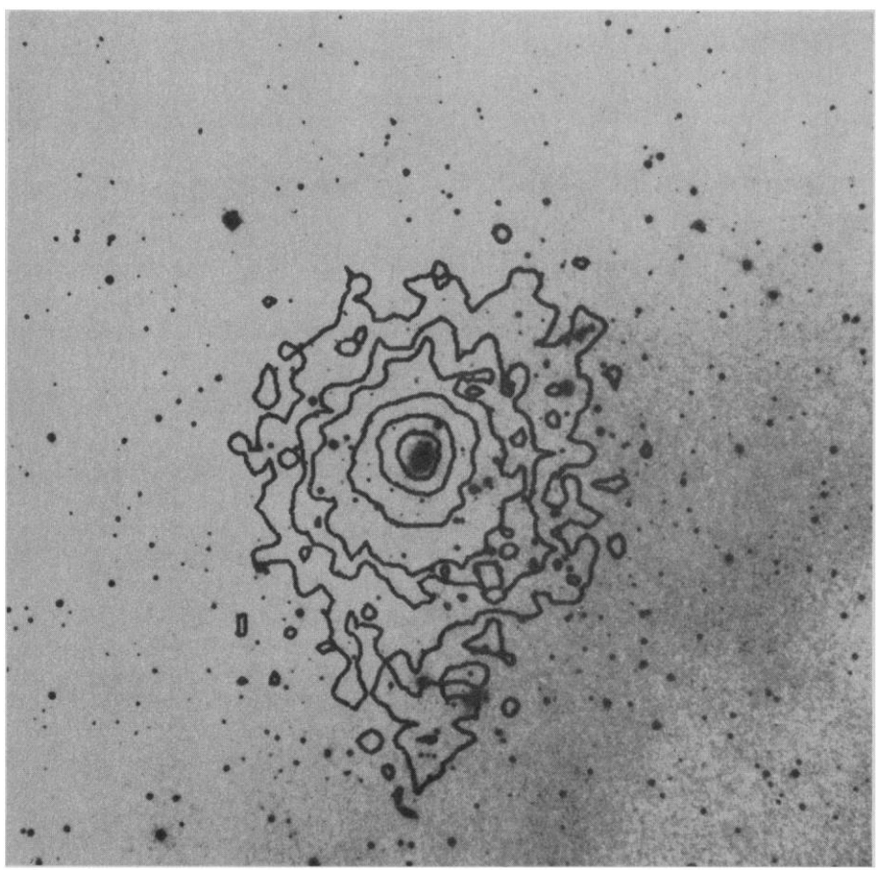

Fig. 11. Isointensity contour map of IPC x-ray data for cluster Abell 85 superimposed on visible light photograph. Note the bright, central galaxy and the highly peaked, smooth x-ray distribution. [This figure originally appeared in *Astrophysical Journal*]

Origin of the X-ray Background and Cosmological Research

The application of x-ray observations to the study of cosmological problems has been a tantalizing possibility since the very beginning of x-ray astronomy. The rocket flight that discovered extrasolar x-ray sources in 1962 (*32*) also discovered the existence of an apparently isotropic background of radiation in the energy range 2 to 8 keV. The results were immediately compared to the predictions of the hot-universe model of steady-state cosmology and were found to be incompatible. At energies below 1 keV, rocket experiments showed the presence of a structured galactic component of the background, while the results of the UHURU and other satellite observations made it clear that at higher energies the background was primarily extragalactic.

Once this was established, it was shown that a substantial fraction of the radiation must originate at redshifts greater than 1 (*33*). Even in the extreme assumption of a uniform distribution of sources in a Euclidean universe, this fraction is greater than 20 percent. Therefore, the study of the cosmic x-ray background may provide information about the early epochs of the universe, particularly in the range of redshifts intermediate between those accessible to optical observations ($z \leq 3$) and those from which the observed microwave background radiation appears to originate ($z \geq 1000$). It is in this intermediate range of redshifts that we may hope to study the transition from density enhancements in a largely homogeneous universe to the first stages of formation and evolution of stellar and/or galactic systems.

Until the advent of the Einstein Observatory we could not, however, use this powerful new tool of cosmological research because we did not understand the origin of the x-ray background radiation and we did not have the sensitivity to observe directly the x-ray emission of even the most powerful extragalactic objects at large redshifts. The great improvement in sensitivity as well as angular resolution brought about by the Einstein mission has given us the opportunity to attack the problem along two distinct, but complementary, lines. The

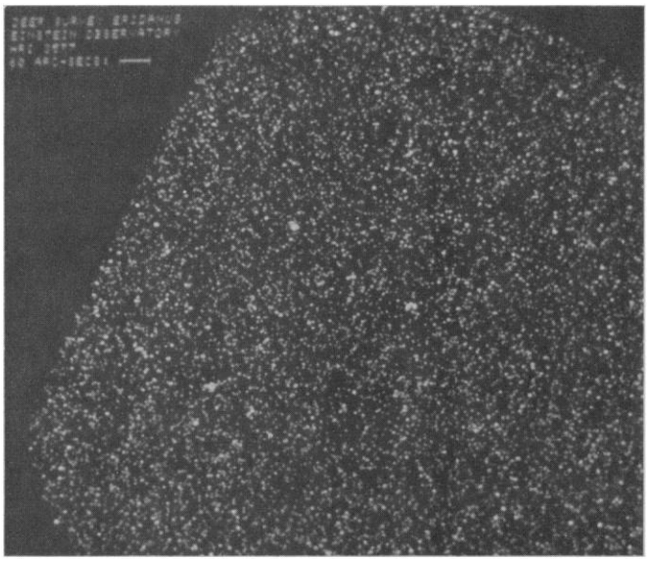

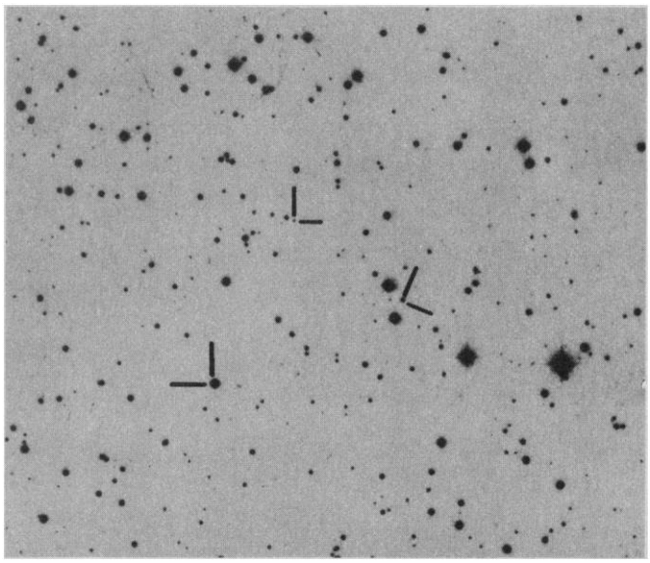

Fig. 12 (left). An HRI image obtained during Einstein deep x-ray survey of field in Eridanus. Three sources—two quasars and one star—are visible in the x-ray data. Fig. 13 (right). Forty-eight-inch Schmidt plate showing the visible light photograph corresponding to the x-ray exposure of Fig. 12. The optical counterparts of the three x-ray sources are indicated.

first is to ascertain directly whether the x-ray background is due to a collection of unresolved individual sources or to truly diffuse processes. The second is to study the x-ray emission from individual classes of sources back to the largest redshifts at which they have been detected and to compare their summed contribution to the total background flux.

The first approach was needed because the data from earlier satellites did not provide sufficient constraints to decide the issue. The observed granularity of the background (~ 3 percent) and its spectrum could be reconciled with either of two hypotheses: that the background was due to the superposition of individual sources or that it was due to a single diffuse emission process. Although the totality of the background could not be explained in terms of any known class of extragalactic emitter without taking into consideration evolutionary effects, once such effects were taken into account, several classes of objects could yield a large fraction, if not all, of the background (*34*).

Among a number of plausible theories that were advanced, the view that the background was due to thermal bremsstrahlung emission from a hot intergalactic plasma appeared most attractive (*35*) and seemed to be supported by the results of HEAO-1 experiments (*36*). Boldt *et al.* (*36*) confirmed and refined previous work on the spectrum of the background and showed that to a high degree of accuracy it appeared to follow an exponential law, as would be predicted for thermal bremsstahlung emission from a gas with a temperature of 45 keV, or 500×10^6 K. For gas that was not excessively clumped, it could be shown that the mass associated with the gas could exceed the mass of every other component of the universe and, in fact, provide a non-negligible fraction of the mass required to slow down and eventually reverse the present expansion of the universe. In spite of the apparent attractiveness and simplicity of this explanation, several problems remained unresolved regarding the origin and heating mechanisms of the gas; in addition, such an explanation limited the contribution from discrete extragalactic sources, contrary to expectation (*37*).

The deep surveys carried out with the Einstein Observatory address this problem by extending the number-intensity relationship to intensities three orders of magnitude fainter than those detected by UHURU, or in other words by directly imaging the background (*38*). If the number of sources increased with decreasing intensity according to a 3/2 power law, as expected for a uniform distribution of sources in a Euclidean universe, we would observe several million sources in the sky or several tens of sources per square degree. At this source density, imaging is essential to avoid source confusion.

We select regions of the sky that have no known x-ray source or peculiar radio or optical features. This is to ensure that they represent as unbiased a sample of the sky as we can choose. We obtain radio and optical coverage of the regions at the very limit of ground-based telescopes and then cover the regions with a mosaic of x-ray exposures. Using automated detection algorithms to reveal the presence of sources, we cross-correlate the information from different detectors or exposures to ascertain the existence of these sources. We then attempt first-cut identifications to determine the galactic or extragalactic nature of the objects. An example is given in Figs. 12 and 13, where the x-ray image and optical photograph of a small region of the sky are shown. The three x-ray sources that can be seen are identified with visible light counterparts, marked by arrows on the 48-inch Schmidt plate. Two of the objects are newly discovered quasars and one a sunlike star, a few hundred light-years away. The quasars are at redshifts of 0.5 and 1.96, respectively.

This example is typical of the findings in the two deep-survey regions analyzed to date. Some of the objects (about one-third) turn out to be stars; the remainder are extragalactic, and of these several are identified with quasars. The survey of the number count of sources indicates that at least 30 percent of the extragalactic background is due to discrete sources, up to our current limit of sensitivity. It is not too daring to surmise that if one could image even fainter sources, perhaps all of the background could be resolved into individual discrete sources. The data are consistent with the view that the bulk of the sources may be quasars at redshifts greater than 1, in agreement with what we could expect from our knowledge of quasar evolutionary effects.

This view is very much strengthened by the complementary study of x-ray emission from quasars at large redshifts

(*39*). Only three quasars, among the nearest to us, had been detected before the launch of Einstein. The Einstein x-ray telescope has made it possible to extend the detection of quasar x-ray emission to the most distant known objects, up to redshifts of 3.5. Our studies show that the average ratio of x-ray to visible light luminosity of these objects, although varying by as much as 250 from object to object, remains fairly constant, independent of the visible light luminosity or the redshift of the object. Then the known increase in the number density of quasars in the past (or at large redshift) can account for all of the x-ray background. In fact, a simple extrapolation based on the observed population of quasars at faint optical magnitudes and on an assumed constant ratio of x-ray to visible luminosity can quickly exceed the observed background. This implies that at some point in the past the quasars have to become weaker in x-rays in proportion to visible light than they are at present, or that the quasar number density must eventually decrease, or both. This is the first important result on cosmological evolution to stem directly from the x-ray data.

We mentioned another example of cosmological research in progress—the search for evolutionary effects in clusters of galaxies. Complete studies of the x-ray properties of clusters at redshifts greater than 1 will probably require advanced x-ray facilities.

Finally, there appears to be within our grasp the prospect, not yet fully realized, of measuring some of the fundamental constants such as the rate of expansion and the age of the universe through a combination of microwave and x-ray measurements of distant clusters (*40*). The main difficulty, in this most important and far-reaching undertaking, is the measurement of the microwave portion of the effect.

These examples should demonstrate that x-ray astronomy has been established through the Einstein observations as a powerful tool for cosmological research. Future progress in these areas, as in many areas of astronomy, will require the combination of sensitivity radio, optical, and x-ray studies.

References and Notes

1. H. Wolter, *Ann. Phys.* **10**, 94 (1952).
2. R. Giacconi and B. Rossi, *J. Geophys. Res.* **64**, 773 (1960).
3. G. S. Vaiana, J. M. Davis, R. Giacconi, A. S. Krieger, J. K. Silk, A. F. Timothy, M. Zombeck, *Astrophys. J. Lett.* **185**, L47 (1973).
4. R. Giacconi *et al.*, *ibid.* **230**, 540 (1979). (This paper furnishes a more detailed description of the Einstein instrumentation and references even more detailed descriptions of the individual instruments.)
5. S. E. Strom, K. M. Strom, G. L. Grasdalen, *Annu. Rev. Astron. Astrophys.* **13**, 187 (1975).
6. T. P. Snow and D. C. Morton, *Astrophys. J. Suppl.* **32**, 429 (1976).
7. H. Tananbaum, in *X- and Gamma-Ray Astronomy*, H. Bradt and R. Giacconi, Eds. (Reidel, Dordrecht, Netherlands, 1973), pp. 9–28.
8. R. Giacconi, in *Proceedings of the 16th Solvay Conference on Physics* (Editions de l'Université de Bruxelles, Brussels, 1974), pp. 27–72.
9. J. Grindlay *et al.*, *Astrophys. J. Lett.* **205**, L127 (1976).
10. G. Garmire, "Low luminosity galactic x-ray sources," *Proceedings of the COSPAR Symposium, Innsbruck, Austria, 29 May to 10 June 1978*.
11. G. Vaiana, *Proceedings of the International Astronomical Union meeting, August 1979, Montreal* (in press).
12. F. R. Harnden *et al.*, *Astrophys. J. Lett.* **234**, L51 (1979).
13. W. Ku and G. Chanan, *ibid.*, p. L59.
14. F. Seward, W. Forman, R. Giacconi, R. E. Griffiths, F. R. Harnden, Jr., C. Jones, J. P. Pye, *ibid.*, p. L55.
15. F. R. Harnden *et al.*, *Bull. Am. Astron. Soc.* **11**, 789 (1980).
16. D. Helfand, G. Chanan, R. Novick, *Nature (London)* **283**, 337 (1980).
17. S. S. Murray, G. Fabbiano, A. C. Fabian, A. Epstein, R. Giacconi, *Astrophys. J. Lett.* **234**, L69 (1979).
18. R. H. Becker, S. S. Holt, B. W. Smith, N. E. White, E. A. Boldt, R. F. Mushotzky, P. J. Serlemitsos, *ibid.*, p. L73.
19. D. Arnett, private communication.
20. D. Weedman, *Annu. Rev. Astron. Astrophys.* **15**, 69 (1977).
21. K. S. Long and D. J. Helfand, *Astrophys. J. Lett.* **234**, L77 (1979).
22. L. Van Speybroeck, A. Epstein, W. Forman, R. Giacconi, C. Jones, W. Liller, L. Smarr, *ibid.*, p. L45.
23. E. J. Schreier, E. Feigelson, J. Delvaille, R. Giacconi, J. Grindlay, D. A. Schwartz, A. C. Fabian, *ibid.*, p. L39.
24. R. J. Dufour and S. van den Bergh, *ibid.* **226**, L73 (1978).
25. D. Lynden-Bell, *Nature (London)* **233**, 690 (1969).
26. M. Elvis, E. Feigelson, R. E. Griffiths, J. P. Henry, H. Tananbaum, in *Highlights of Astronomy* (Reidel, Dordrecht, Netherlands, in press).
27. H. Gursky, E. Kellogg, S. Murray, C. Leong, H. Tananbaum, R. Giacconi, *Astrophys. J. Lett.* **167**, L81 (1971).
28. W. Forman *et al.*, *ibid.* **234**, L27 (1979).
29. A. C. Fabian, J. Schwarz, W. Forman, in preparation.
30. C. Jones, E. Mandel, J. Schwarz, W. Forman, S. S. Murray, F. R. Harnden, Jr., *Astrophys. J. Lett.* **234**, L21 (1979).
31. J. P. Henry, G. Branduardi, U. Briel, D. Fabricant, E. Feigelson, S. S. Murray, A. Soltan, H. Tananbaum, *ibid.*, p. L15.
32. R. Giacconi, H. Gursky, F. Paolini, B. Rossi, *Phys. Rev. Lett.* **9** (No. 11), 439 (1962).
33. D. Schwartz and H. Gursky, in *X-ray Astronomy*, R. Giacconi and H. Gursky, Eds. (Reidel, Dordrecht, Netherlands, 1974), pp. 359–388.
34. D. Schwartz, in *(COSPAR) X-Ray Astronomy*, W. Baity and L. E. Peterson, Eds. (Pergamon, New York, 1979), pp. 453–465.
35. G. Field, *Annu. Rev. Astron. Astrophys.* **10**, 227 (1972).
36. E. Boldt, F. Marshall, R. Mushotzky, S. Holt, R. Rothschild, P. Serlemitsos, in *COSPAR X-ray Astronomy*, W. A. Baity and L. E. Peterson, Eds., (Pergamon, New York, 1979), p. 443.
37. G. Field, in preparation.
38. R. Giacconi *et al.*, *Astrophys J. Lett.* **234**, L1 (1979).
39. H. Tananbaum *et al.*, *ibid.*, p. L9.
40. J. Silk and S. D. M. White, *ibid.* **226**, L103 (1978).

41. We gratefully acknowledge the help of hundreds of engineers, scientists, students, program managers, computer programmers, technicians, and secretaries, without whose contributions the Einstein program would not have been possible. Although it is not possible to acknowledge individuals, we wish to take this opportunity to recognize the organizations to which they belong. The help and support of NASA Headquarters, the guidance by the management team led by F. Speer at Marshall Space Flight Center, the support by Kennedy Space Flight Center for launch, and the ongoing team efforts at Goddard Space Flight Center for mission operations have been essential. Also essential were the efforts of the industrial contractors: TRW for the spacecraft design and construction; AS & E for the experiment construction, integration, and testing; Perkin-Elmer for the fabrication of the x-ray mirror; Honeywell Electro-Optics Center for the construction and testing of the star trackers; Convair Division General Dynamics for the construction of the optical bench; LND for the preparation of proportional counters; Parker-Hannifin Corp., Lord Corp., Aeroflex Laboratories, Inc., R & K Precision Machine Co., and Astronautic Industries, Inc. for many of the mechanical assemblies; Spacetac, Inc. and Matrix Research and Development Corp. for low- and high-voltage power supplies; and, finally BASD (formerly Ball Brothers) for the construction of the cryostat. We wish to acknowledge the constant support given to this project by the management and staff of our own institutions: Harvard/Smithsonian Center for Astrophysics (R. Giacconi, Principal Investigator; Harvey Tananbaum, Scientific Program Manager; Leon Van Speybroeck, assumed scientific guidance for design and development of the grazing incidence telescope); Massachusetts Institute of Technology (George W. Clark, Principal Scientist); Goddard Space Flight Center (Stephen S. Holt, Principal Scientist); and Columbia University (Robert Novick, Principal Scientist). This research was sponsored under NASA contracts NAS8-30751, NAS8-30752, and NAS8-30753.